## Title

PROTON-H2 SCATTERING ON AN AB INITIO CI POTENTIAL ENERGY SURFACE I: VIBRATIONAL EXCITATION AT 10 eV



## Author

Schinke, R.

## Publication Date

1979-12-01

LBL-9421 c.1
Preprint

NRCC NATIONAL RESOURCE FOR COMPUTATION IN CHEMISTRY

Submitted to the Journal of Chemical Physics

# PROTON-$H_2$ SCATTERING ON AN AB INITIO CI POTENTIAL ENERGY SURFACE I: VIBRATIONAL EXCITATION AT 10 eV

R. Schinke, M. Dupuis and W. A. Lester, Jr.



December 1979



LAWRENCE BERKELEY LABORATORY
UNIVERSITY OF CALIFORNIA, BERKELEY



Prepared for the U.S. Department of Energy under Contract W-7405-ENG-48

## DISCLAIMER

# PROTON-$H_2$ SCATTERING ON AN AB INITIO CI POTENTIAL ENERGY SURFACE I: VIBRATIONAL EXCITATION AT 10 eV

R. Schinke*

Fachbereich Physik, Universität Kaiserslautern
675 Kaiserslautern, FRG
and
IBM Research Laboratory, 5600 Cottle Road, San Jose, CA 95193

M. Dupuis† and W. A. Lester, Jr.*†

National Resource for Computation in Chemistry
Lawrence Berkeley Laboratory, University of California
Berkeley, California 94720
and
IBM Research Laboratory, 5600 Cottle Road, San Jose, CA 95193

## ABSTRACT

A complete configuration interaction (CI) ground state surface for the $H_3^+$ system has been calculated using 5S and $3(P_x,P_y,P_z)$ basis functions at each center. A total of 650 nuclear geometries has been considered which makes the new surface appropriate not only for scattering calculations, but also for the evaluation of the vibrational-rotational spectrum of the $H_3^+$ molecule. Significant deviations are found from the analytic Giese and Gentry potential used in many previous theoretical studies, especially for large and small non-equilibrium H-H separations which are important for vibrational excitation of the $H_2$ molecule. Vibrational-rotational excitation cross sections have been calculated in the rotational sudden approximation where the vibrational degree of freedom is treated exactly by solving seven vibrationally coupled radial equations. The use of the new surface leads to increased vibrational excitation compared to previous calculations utilizing the same scattering

approximation and to excellent agreement at 10 eV with the angle-dependent measurements of Hermann, Schmidt and Linder.

---

*Research supported in part by the U. S. Office of Naval Research.
†Research supported in part by the National Resource for Computation in Chemistry under a grant from the National Science Foundation and the Basic Energy Sciences Division of the U. S. Department of Energy under Contract No. W—7405-ENG-48.

## I. INTRODUCTION

In a recent study[1] combined vibrational-rotational excitation cross sections for nonreactive proton-$H_2$ collisions were calculated at collision energies E = 4.67 eV and 10 eV. The infinite-order-sudden (IOS) approximation for rotational motion was used. The vibrational degree of freedom of the $H_2$ molecule was treated exactly by solving the vibrationally coupled equations for the radial wavefunctions. For detailed discussion and background, see Refs. 1 and 2. The analytic potential of Giese and Gentry,[3] which is a fit to 138 ab initio configuration interaction (CI) energies of Csizmadia, et al.,[4] was used in both of these studies. Comparisons with highly resolved experimental data[5,6] were generally satisfactory, although some significant deviations were found: (a) the theoretical transition probabilities for vibrational excitation as a function of scattering angle were too small; (b) the differential cross sections for the $j = 1 \rightarrow j' = 3$, 5 and 7 rotational transitions in the vibrational ground state exhibited very strong rainbow maxima not observed in the experiments. Surprisingly, the rigid-rotor calculations of McGuire et al.[7-9] gave better agreement with the experimental rotational transition probabilities than the full vibrational-rotational calculations of Ref. 1.

On the theoretical side there are two possible sources for the reported deviations: the IOS approximation and the potential energy surface. A comparison of rotational excitation differential cross sections calculated in the rigid-roter approximation with the more

accurate coupled-states results of McGuire[7] confirmed the applicability of the IOS treatment for the present system for energies above ~4 eV and rotational transitions up to $\Delta j = 6$.[2] Therefore, we believe that for $H^+$-$H_2$ at the energies considered the IOS approximation is capable of quantitative predictions that lie within present experimental uncertainties. It becomes more evident that differences between experiment and theory are due to the potential energy surface, when one considers that three scattering calculations, following different formalisms that make use of the same potential energy surface, give almost the same vibrational transition probabilities at 10 eV. Here we refer to (a) the semi-classical DECENT calculations of Ref. 3, (b) the impact-parameter calculations of Refs. 10 and 11, and (c) the vibrotor IOS calculations of Ref. 1. At higher collision energies details of the potential gradually become less important so that at $E_{cm}$ = 20 eV time-dependent calculations[11,12] are in good agreement with measurements.

The Giese and Gentry (GG) potential function was constructed using ab initio CI energies computed at geometries pertinent to reactive scattering of $H^+$ by $H_2$. Previous convergence studies[10] showed that at least the lowest four vibrational states are needed in the vibrationally close-coupled calculations to achieve reliable $n = 0 \rightarrow n' = 1$ and 2 vibrational excitation cross sections. However, vibrational motion in these states samples regions of the potential for $0.6\ a_o \lesssim R_{HH} \lesssim 2.6\ a_o$, a regime which is not assured to be adequately described by the GG potential. One notes, however, that

the ab initio CI energies used by GG are sufficiently accurate for most scattering applications and that the fit expression has an average error of less than 0.5 kcal/mol.[3]

The goal of this study is to present the results of extensive ab initio CI calculations including 650 geometries which cover the whole configuration space necessary for vibrational-rotational excitation. With the availability of this new potential energy surface, differences in scattering calculations can be discussed in terms of differences in potential energy surfaces which should be useful in establishing the accuracy of a surface necessary for quantitative agreement between theory and experiment. In Section II we describe the potential energy surface calculation, and in Section III we discuss the procedure used to fit the CI energies. Finally, in Section IV we present scattering results obtained using the present surface and compare them with the theoretical results of Ref. 1 and with measurements.

## II. AB INITIO CI CALCULATIONS

There exist many electronic structure calculations for the $H_3^+$ system.[4,13-15] Carney and Porter,[13] Dykstra et al.,[14] and Dykstra and Swope[15] were mainly interested in the calculation of the spectroscopic constants of $H_3^+$. Therefore, they considered only the well region and, consequently, their calculations are not very helpful for scattering applications. On the other hand, Czismadia et al.[4] were interested in low energy $H^+$-$H_2$ reactions and calculated ab initio CI energies over a range of geometries that led to the speculation, mentioned in the introduction, on whether the range they explored is adequate for the relatively high (n = 4) vibrational excitation regime of interest here.

We performed a complete CI calculation in the space spanned by 5S- and 3P-type Gaussian basis functions located at each center. This procedure leads to 42 basis-functions and 606 A' configurations. The exponents of the S functions were taken from Huzinaga[16] and the exponents of the three P functions were determined by an even-tempered optimization, $\alpha_1 = \alpha x$, $\alpha_2 = \alpha$ and $\alpha_3 = \alpha/x$, with $\alpha = 0.7$ and $x = 2.25$; hence $\alpha_1 = 1.575$, $\alpha_2 = 0.7$, and $\alpha_3 = 0.311$. The optimization was done at an equilateral geometry with an internuclear separation of 1.66 $a_o$, as in Ref. 6, giving an energy of -1.3402295 hartrees compared to -1.3373 hartrees obtained by Czismadia et al.[4] The absolute minimum of the ground state surface is not at this geometry but it is very close to it. Dykstra et al.[14] used 63 basis functions in a complete CI wavefunction and determined the minimum to

be -1.342284 hartrees for an equilateral geometry with internuclear separation of 1.6500 $a_o$. Carney and Porter[13] found the minimum at the same geometry and an energy of -1.339358 hartrees. The total energy of the $H_2$ molecule at $R_{H-H} = 1.4\ a_o$ obtained in this work is -1.1715303 hartrees compared to the exact value of -1.174470 hartrees of Kolos and Wolniewicz.[17] Czismadia et al.[4] calculated the minimum at the same geometry to be -1.1668 hartrees whereas Dykstra et al.[14] obtained -1.173387 hartrees. Carney and Porter[13] did not report the energy at this distance.

The following brief comparison illustrates the accuracy of our ab initio CI calculation. With respect to the total minimum our calculations were ~1.8 kcal/mol below those of Czismadia et al.,[4] who used a smaller atomic basis set and a limited electronic configuration basis. Dykstra et al.[14] included an additional d function in their complete CI calculation and calculated energies ~1.6 kcal/mol below ours. These basis set differences certainly have an effect on the computed spectroscopic constants for the $H_3^+$ molecule derived from the various potentials, however, we believe that our calculated potential energy surface is accurate enough for scattering calculations at collision energies of several electron volts. As discussed in the introduction, it is far more important to have carefully sampled the surface with a large number of geometries to cover the whole configuration space necessary for scattering calculations than to have sought energy improvements beyond the present level.

The most convenient coordinates for non-reactive collisions are R, the distance between the proton and the midpoint of $H_2$, r, the H-H separation, and $\gamma$, the angle formed by $\vec{R}$ and $\vec{r}$. To select the geometries $(R_i, r_j, \gamma_k)$ at which the CI calculations were performed, we varied the three coordinates systematically within the boundaries: $0 \leq R \leq 10\ a_o$, $0.6\ a_o \leq r \leq 2.6\ a_o$ and $0^o \leq \gamma \leq 90^o$. The following values $R_i$, $r_j$, $\gamma_k$ were chosen:

(1)

$R_i$ = 0, 0.3, 0.5, 0.75, 1.0, 1.25, 1.5, 1.75, 2.0, 2.25, 2.5, 2.75, 3.0, 3.25, 3.5, 4.0, 5.0, 6.0, 8.0, 10.0 $a_o$ $\quad i = 1, \ldots, 20$

$r_j$ = 0.6, 1.0, 1.4, 1.8, 2.2, 2.6 $a_o$ $\quad j = 1, \ldots, 6$

$\gamma_k = 0^o, 18^o, 36^o, 54^o, 72^o, 90^o \quad k = 1, \ldots, 6,$

giving 720 geometries $(R_i, r_j, \gamma_k)$. Actually, 650 energy values were calculated. The complete listing of the potential energy surface is available upon request from one of us (R.S.).

## III. ANALYTICAL EXPRESSION FOR THE SURFACE

In non-reactive scattering calculations the interaction potential $V_I(R,r,\gamma)$ is needed rather than the total potential energy $V(R,r,\gamma)$. The interaction potential at each geometry $(R_i,r_j,\gamma_K)$ is defined by

$$V_I(R_i,r_j,\gamma_k) = V(R_i,r_j,\gamma_k) - V(R=\infty,r_j,\gamma_k) \quad . \quad (2)$$

It is well known that the ground state of $H_3^+$, which dissociates into $H^+ + H_2$, has an avoided crossing at $r \sim 2.5\ a_o$ with the second state of the same symmetry which dissociates into $H + H_2^+$. The energy splitting is very small at large separations of the two subsystems and, consequently, both potentials show a sharp cusp-like behavior as functions of the H-H and $H-H^+$ separations. As the two subsystems approach each other this splitting increases and both potential curves gradually become smoother as shown in Ref. 18. At $R = 4\ a_o$, for example, the splitting is so large that the characteristics of the avoided crossing have totally vanished. This raises the question whether a diabatic or an adiabatic representation is appropriate for the study of pure inelastic transitions, i.e., when reactive and charge-transfer processes are excluded. We follow the reasoning of Giese and Gentry[3] and consider the system to be diabatic for large $R(\gtrsim 4\ a_o)$ and adiabatic for small $R(\lesssim 4\ a_o)$.

This distinction, of course, is only meaningful for $r \gtrsim 2.5\ a_o$. The definition in Eq. (2) is unique for $r \leqslant 2.5\ a_o$; both $V(R,r,\gamma)$

and $V(R=\infty,r,\gamma)$ represent the lower surface. Only for $j = 6$, $r_{j=6} = 2.6\ a_o$, does Eq. (2) have to be modified in the following sense:

$$V_I(R_i,r_j,\gamma_k) = V(R_i,r_j,\gamma_k) - [1 - \omega(R_i)]\ V^{lower}(R = \infty,r_j,\gamma_k) \qquad (3)$$

$$- \omega(R_i)\ V^{upper}\ (R = \infty, r_j, \gamma_k) \text{ only for } j = 6,$$

with

$$\omega(R) = 1 \qquad \text{for } R \leqslant 4$$

$$\omega(r) = \exp\left[-0.3(R - 4.0)^2\right] \qquad \text{for } R \geqslant 4 \qquad (4)$$

For large R ($\omega \sim 0$) the asymptotic limit of the lower surface (ground state) is subtracted from the ground state, while for small R ($\omega = 1$) the asymptotic limit of the upper surface is subtracted. The function $\omega(R)$ has been introduced to achieve a smooth change from the diabatic to the adiabatic region. As the asymptotic potentials $V^{lower}$ and $V^{upper}$ we take the first two roots of the CI calculations rather than the exact ones.

The interaction potential, Eq. (2), is shown in Fig. 1 as a function of R for the collinear, $\gamma = 0^{o}$, and the perpendicular, $\gamma = 90^{o}$, geometries and for three selected r-values. The open circles are the computed CI energies and the solid line represents the analytic fit, which will be discussed below. The closed circles are calculated from GG's potential. They are not included for $r = 0.6\ a_o$ since the deviation from the present CI energies is very large at this distance for reasons that will be discussed below. For collinear geometry the well is shifted to larger R values as r is increased, while in the perpendicular approach the reverse is found, although to a lesser extent. The differences between the present CI energies and GG's values are smallest for $r = 1.4\ a_o$ around the minimum of the well. This is not surprising because Czismadia et al.[4] calculated more CI energies in this region than in any other region to determine the minimum energy path.

When all three nuclei are close together, the internuclear separations $\bar{R}_i$ (i = 1,2,3) are more appropriate for describing the potential energy surface than the coordinates R, r, and $\gamma$. All CI energies for $R \leq 4.0\ a_o$ and $V(R,r,\gamma) \leq -0.1$ hartrees have been used in a least squares procedure to determine the linear coefficients in the expression

$$V_I^{FIT}(\bar{R}_1,\bar{R}_2,\bar{R}_3) = \sum_{\nu=1}^{23} \Big[ a_\nu \phi_\nu(S_1,S_2,S_3)\, e^{-1.0(S_1+S_2+S_3)} + b_\nu \phi_\nu(S_1,S_2,S_3)\, e^{-0.25(S_1+S_2+S_3)^2} \Big] \qquad (5)$$

$$+ z_1(\bar{R}_1^{-4} + \bar{R}_2^{-4}) + \bar{R}_3^{-4}) + z_2(\bar{R}_1^{-6} + \bar{R}_2^{-6} + \bar{R}_3^{-6})$$

$$+ z_3(\bar{R}_1^{-8} + \bar{R}_2^{-8} + \bar{R}_3^{-8}) + z_4(\bar{R}_1^{-10} + \bar{R}_2^{-10} + \bar{R}_3^{-10})$$

with $S_i = \bar{R}_i - 0.75\ a_o$ $(i = 1,2,3)$. The functions $\phi_\nu(S_1,S_2,S_3)$ are polynomials of up to sixth order and because of the symmetry of the $H_3^+$ system, symmetric in all three variables. They are given in Table I together with the coefficients $a_\nu$, $b_\nu$ and $z_k$ ($\nu = 1, \ldots, 23$, $k = 1, \ldots, 4$). The condition $V(R,r,\gamma) \leqslant -0.1$ hartrees eliminates energies ~25 eV above the $H + H + H^+$ dissociation limit which would unnecessarily complicate the fitting. The average deviation of $V_I^{FIT}$ from the 443 CI energies computed in the region of validity of Eq. (5) is 0.13 kcal/mol.

In the region $2.0\ a_o \leqslant R \leqslant 8.0\ a_o$, an interpolation procedure was applied which exactly reproduces the present CI energies. For each set $(r_j,\gamma_k)$ $(j, k = 1, \ldots, 6)$ the R-dependence of the interaction potential is expressed as a cubic spline function

$$V_I^{INT}(R,r_j,\gamma_k) = A_{jk}^{(i)} + B_{jk}^{(i)}(R-R_i) + C_{jk}^{(i)}(R-R_i)^2 + D_{jk}^{(i)}(R-R_i)^3 \qquad (6)$$

for $R_i \leq R \leq R_{i+1}$. The 6 x 6 coefficient matrices $\underline{\underline{A}}^{(i)}$, $\underline{\underline{B}}^{(i)}$, $\underline{\underline{C}}^{(i)}$, and $\underline{\underline{D}}^{(i)}$ for all i have to be calculated only once. The evaluation of the interpolation potential $V_I^{INT}$ at any arbitrary geometry $(R,r,\gamma)$ proceeds as follows: (1) For each $(r_j,\gamma_k)(j,k = 1,\ldots,6)$ calculate $V_I^{INT}(R,r_j,\gamma_k)$ according to Eq. (6) which gives 36 potential values. (2) For each angle $\gamma_k$ make a second cubic spline interpolation in the variable r similar to Eq. (6). (3) The resulting 6 values $V_I^{INT}(R,r,\gamma_k)$ $(k = 1,\ldots,6)$ are used to determine the 6 coefficients $p_k$ in an expansion in Legendre polynomials

$$V_I^{INT}(R,r,\gamma) = \sum_{k=1}^{6} p_k P_{2(k-1)}(\cos\gamma) \qquad (7)$$

where, due to the symmetry of the system, only even order Legendre polynomials contribute.

The fit potential $V_I^{FIT}$ is defined for $0 \leq R \leq 4\ a_o$ and the interpolation potential $V_I^{INT}$ is valid for $R \geq 2.0\ a_o$. In order to achieve a smooth and continuous change from the fit region to the interpolation region, the following modification is introduced:

$$V_I(R,r,\gamma) = \omega_1(R)V_I^{FIT}(R,r,\gamma) + \omega_2(R)V_I^{INT}(R,r,\gamma) \qquad (8)$$

with the weighting functions defined by

$$\begin{aligned}
&\omega_1(R) = 1 \quad \text{and} \quad \omega_2(R) = 0 && \text{for } R \leqslant 2\ a_o \\
&\omega_{1(2)}(R) = 1/2 \pm 1/2 \cos(\pi/2\ R - \pi) && \text{for } 2\ a_o \leqslant R \leqslant 4\ a_o \qquad (9) \\
&\omega_1(R) = 0 \quad \text{and} \quad \omega_2(R) = 1 && \text{for } R \geqslant 4\ a_o
\end{aligned}$$

For large proton-$H_2$ distances R, we believe that the interaction potential is better described by the perturbation theory limit[19] (PTH) than by the CI energies. Following GG[3] we set, for $R \geqslant 12\ a_o$,

$$V_I^{PTH}(R,r,\gamma) = -\left[A_0(r) + A_2(r)\ P_2(\cos\gamma)\right] R^{-4} + Q_2(r)\ P_2(\cos\gamma)\ R^{-3} \quad , \qquad (10)$$

where the functions $A_0$, $A_2$ and $Q_2$ are given in Ref. 3 and therefore not repeated here. $P_2$ is the Legendre polynomial of order 2. In order to achieve a potential surface which is continuous and smooth from the interpolation region, $R \leqslant 8\ a_o$, to the perturbation theory region, $R \geqslant 12\ a_o$, we expand the interaction potential for each set $(r_j,\gamma_k)(j,k=1,\ldots,6)$ in an inverse power series in R

$$V_I^{EXP}(R,r_j,\gamma_k) = \sum_{i=1}^{4} E_{jk}^{(i)} R^{-i+1} \qquad (11)$$

where the 6 x 6 coefficient matrices $\underline{\underline{E}}^{(i)}$ (i = 1,...,4) are determined such that $V_I$ and $\partial V_I/\partial R$ are continuous at R = 8 $a_o$ and 12 $a_o$ for each set $(r_j,\gamma_k)$. The evaluation of the potential $V_I^{EXP}$ for arbitrary geometry (8 $a_o \leq R \leq$ 12 $a_o$,r,$\gamma$) then proceeds as previously indicated for the interpolation region except that Eq. (6) is replaced by Eq. (11).

The five different regions of configuration space and the representation of the interaction potential in each of them is schematically summarized in Fig. 2. The procedure used here is definitely more complicated than the construction of a single analytical expression covering the whole configuration space as done, for example, by GG[3]. However, the advantage of our procedure is that in each region the physically most appropriate description is utilized. Thus, the average deviation from the CI energies is only 0.16 kcal/mol over a range of 35 eV--the difference between the minimum and the highest energy taken into account in the fitting procedure. The present function is valid only for 0.6 $a_o \leq r \leq$ 2.6 $a_o$ and in the form given is not suitable for reaction studies.

## IV. SCATTERING RESULTS

As an initial test of this potential energy surface, we have computed integral and differential cross sections for vibrational and rotational excitation at 10 eV collision energy. The infinite-order-sudden approximation for rotational motion was utilized. The vibrational motion was treated explicitly by solving coupled radial equations. Because the calculations reported in this work are identical to those described in detail in Ref. 1, we only report and discuss the results.

Vibrational excitation obviously depends on the vibrational matrix elements

$$V_{nn'}(R,\gamma) = \int_0^\infty dr\, \phi_n(r)\, V_I(R,r,\gamma)\, \phi_{n'}(r) \quad , \qquad (12)$$

which provide the coupling between the various states n, n'. In the rotational sudden approximation these elements depend on the orientation angle $\gamma$. The functions $\phi_n(r)$ are the vibrational eigenfunctions of the target molecule. In Fig. 3 we show the r-dependence of the interaction potential for the collinear arrangement and selected proton-$H_2$ distances, and in Fig. 4 present similar plots for perpendicular geometry. The present CI energies are indicated by closed circles; the solid line is the analytical expression of Section III; and the dashed line is GG's function.

The most striking feature of Figs. 3 and 4 is the qualitative differences of the surfaces for $r \leq 1\ a_o$. Except for $R = 2\ a_o$ and $\gamma = 0^o$, the present potential monotonically increases with decreasing r, while GG's potential shows in general a maximum at $r \sim 1\ a_o$ and rapid decrease for smaller H-H separations. This simply means that the $H_2$ repulsion for small r is weakened by the approaching proton. Such an artifact is not surprising since $1.35\ a_o$ was the smallest $H_2$ distance used by GG to determine their fit expression. Foreseeably, agreement is best for $r = 1.4\ a_o$. Finally, we point out that there are significant deviations even at large proton-$H_2$ distances, so that the contributions from large partial waves, which are most important for cross sections in this charge-neutral system, will also be different. So far it is clear that the differences in the surfaces will result in different cross sections. Due to the complexity of Eq. (12), however, one can not decide <u>a priori</u> whether vibrational excitation will be decreased or increased.

The rotational sudden S-matrix elements for vibrational excitation are extracted from the solutions of the vibrationally coupled equations. For the transition $n = 0 \rightarrow n' = 1$ and an energy of 10 eV these elements are shown in Fig. 5 as a function of the partial wave parameter $\ell'$, the final orbital angular momentum, for the collinear and the perpendicular approaches, respectively. Also shown are the same quantities from Ref. 1 obtained using GG's potential. The general features remain unchanged, strong oscillations at lower partial waves

and a broad maximum at higher partial waves which, due to the $(2\ell' + 1)$ weighting, contribute the most to the cross sections. However, this maximum is strongly enhanced with the potential of this study. The effect is more pronounced for $\gamma = 90^{\circ}$, in accord with Figs. 3 and 4 where the differences between the two surfaces are shown to be largest for perpendicular geometry. Due to the $\sin\gamma$ weighting in the final integration over the orientation angle in the sudden limit,[1] angles $\gamma \approx 90^{\circ}$ make the most important contributions. Consequently, all vibrational excitation cross sections in Table II, summed over all rotational transitions, are larger for the new surface. The $n = 0 \rightarrow 1$ cross section is 47% larger than that of Ref. 1. For $n' = 2$ the change is even larger (81%).

The strongest test of both potential energy surface and scattering theory is provided by comparisons with angle-dependent experimental data. In Fig. 6 we show the probabilities for the vibrational transitions $n = 0 \rightarrow 1,2$, and 3, e.g.,

$$P^{n'}(\theta) = \left[\sum_{j'} \frac{d\sigma}{d\Omega}(0j \rightarrow n'j')\right]\left[\sum_{n''}\sum_{j''} \frac{d\sigma}{d\Omega}(0j \rightarrow n''j'')\right]^{-1} \qquad (13)$$

vs scattering angle $\theta$. Both the theoretical and the experimental results of Hermann et al.[5] are absolute quantities that require no normalization. While the previous calculations[1] with GG's surface significantly underestimated the $n' = 1$ and 2 transitions, the present theoretical results are in excellent agreement with the measurements over the entire range of scattering angles. The situation for $n' = 3$ is not significant since the probabilities are very small, only 2-3% of all scattering events. But even in this case a slight improvement is perceptible.

Hermann et al.[5] also report differential cross sections for the vibrationally elastic and inelastic transitions. In Fig. 7 the experimental results are compared with results of this study and of Ref. 1. The various excitation cross sections have been multiplied by factors of $10^{-1}$ for ease of visualization. Since the experimental differential cross sections are given only in arbitrary units they have been normalized to the theoretical elastic cross section at $\sim 15^{\circ}$. Note that only one normalization point was used for all vibrational transitions. The rainbow angle in the elastic cross section is shifted slightly to the forward direction with the result that the present theoretical curve is in better accord with experiment than the one of Ref. 1. Similar comments hold for all vibrational transitions.

## V. SUMMARY

(1) Significant differences are found for small and large $H_2$ separations between the Giese and Gentry[3] potential surface and the present ab initio CI potential. The shortcomings of the analytical potential of Ref. 3 for collision energies of interest here were found to be due to the lack of CI energies for these regions in its construction.

(2) These differences in potential energy surface result in significant changes in the scattering computed at 10 eV collision energy. The total cross section for vibrational excitation is increased by a factor of 1.5 over the results of Ref. 1 obtained using the potential energy surface of Giese and Gentry.

(3) Using the potential energy surface reported in this paper, the angle-dependent transition probabilities for vibrational excitation are found to be in excellent agreement with the measurements of Hermann et al.[5] In addition, some minor quantitative improvements are found in the differential cross sections including a slight shift of the rainbow maxima to the forward direction.

ACKNOWLEDGEMENTS

R. S. is grateful to the Deutsche Forschungsgemeinschaft for financial support.

REFERENCES

1. R. Schinke and P. McGuire, Chem. Phys. 31, 391 (1978).
2. R. Schinke and P. McGuire, Chem. Phys. 28, 129 (1978).
3. C. F. Giese and W. R. Gentry, Phys. Rev. A10, 2156 (1974).
4. I. G. Czismadia, R. E. Kari, J. C. Polanyi, A. C. Roach and M. A. Robb, J. Chem. Phys. 52, 6205 (1970).
5. V. Hermann, H. Schmidt and F. Linder, J. Phys. B. 11, 493 (1978).
6. H. Schmidt, V. Hermann and F. Linder, J. Chem. Phys. 69, 2734 (1978).
7. P. McGuire, J. Chem. Phys. 65, 3275 (1976).
8. P. McGuire, H. Schmidt, V. Hermann and F. Linder, J. Chem. Phys. 66, 4243 (1977).
9. P. McGuire, H. Schmidt, V. Hermann and F. Linder, Abstracts of the X ICPEAC, Paris (1977).
10. R. Schinke, Chem. Phys. 24, 379 (1977).
11. R. Schinke, H. Krüger, V. Hermann, H. Schmidt and F. Linder, J. Chem. Phys. 67, 1187 (1977).
12. J. Krutein, G. Bischof, F. Linder and R. Schinke, J. Phys. B. 12, L57 (1979).
13. G. D. Carney and R. N. Porter, J. Chem. Phys. 60, 4251 (1974).
14. C. E. Dykstra, A. S. Gaylord, W. D. Gwinn, W. C. Swope, and H. F. Schaefer III, J. Chem. Phys. 68, 3951 (1978).
15. C. E. Dykstra and W. C. Swope, J. Chem. Phys. 70, 1 (1979).
16. S. Huzinaga, J. Chem. Phys. 42, 1293 (1965).
17. W. Kolos and L. Wolniewicz, J. Chem. Phys. 41, 3663 (1964); J. Mol. Spectrosc. 54, 303 (1975).

18. C. W. Bauschlicher, Jr., S. V. O'Neil, R. K. Preston, H. F. Schaefer, III and C. F. Bender, J. Chem. Phys. 59, 1286 (1973).

19. A. D. Buckingham. Adv. Chem. Phys. 12, 107 (1967).

Table I. Polynomials $\phi_\nu$, coefficient $a_\nu$ and $b_\nu$ and other parameters used in Eq. (5).*

| $\nu$ | $\phi_\nu$ | $a_\nu$ | $b_\nu$ |
|---|---|---|---|
| 1 | 1 | 0.443996(3) | -0.444132(3) |
| 2 | $s_1+s_2+s_3$ | 0.170068(3) | 0.273644(3) |
| 3 | $s_1^2+s_2^2+s_3^2$ | -0.671525(2) | -0.952916(2) |
| 4 | $s_1s_2+s_2s_3+s_1s_3$ | 0.427881(2) | -0.146967(3) |
| 5 | $s_1^3+s_2^3+s_3^3$ | -0.335414(2) | 0.234512(2) |
| 6 | $s_1s_2^2+s_2s_1^2+s_2s_3^2+s_3s_2^2+s_3s_1^2+s_1s_3^2$ | -0.331219(2) | 0.447606(2) |
| 7 | $s_1s_2s_3$ | 0.816418(1) | 0.555559(2) |
| 8 | $s_1^4+s_2^4+s_3^4$ | 0.294849(1) | -0.298710(1) |
| 9 | $s_1s_2^3+s_2s_1^3+s_2s_3^3+s_3s_2^3+ s_3s_1^3+s_1s_3^3$ | -0.973540(1) | -0.100774(2) |
| 10 | $s_1^2s_2^2+s_2^2s_3^2+s_3^2s_1^2$ | 0.345336(1) | -0.828151(1) |
| 11 | $s_1s_2s_3^2+s_1s_2^2s_3+s_1^2s_2s_3$ | -0.762486(1) | -0.135837(2) |
| 12 | $s_1^5+s_2^5+s_3^5$ | 0.239269(1) | 0.253210 |
| 13 | $s_1s_2^4+s_2s_1^4+s_2s_3^4+s_3s_2^4+s_3s_1^4+s_1s_3^4$ | 0.375664(1) | 0.113737(1) |
| 14 | $s_1^2s_2^3+s_2^2s_1^3+s_2^2s_3^3+s_3^2s_2^3+s_3^2s_1^3+s_1^2s_3^3$ | 0.555669(1) | 0.125204(1) |
| 15 | $s_1s_2s_3^3+s_1s_2^3s_3+s_1^3s_2s_3$ | 0.410436(1) | 0.220384(1) |
| 16 | $s_1s_2^2s_3^2+s_1^2s_2s_3^2+s_1^2s_2^2s_3$ | 0.119800(2) | 0.185953(1) |
| 17 | $s_1^6+s_2^6+s_3^6$ | -0.336222 | 0.176020(-1) |
| 18 | $s_1s_2^5+s_2s_1^5+s_2s_3^5+s_3s_2^5+s_3s_1^5+s_1s_3^5$ | -0.215168 | -0.134948 |
| 19 | $s_1^2s_2^4+s_2^2s_1^4+s_2^2s_3^4+s_3^2s_2^4+s_3^2s_1^4+s_1^2s_3^4$ | -0.842516 | 0.102925 |
| 20 | $s_1^3s_2^3+s_2^3s_3^3+s_3^3s_1^3$ | -0.626637 | -0.277897 |
| 21 | $s_1s_2s_3^4+s_1s_2^4s_3+s_1^4s_2s_3$ | -0.110029(1) | -0.123250 |
| 22 | $s_1s_2^2s_3^3+s_1s_2^3s_3^2+s_1^2s_2s_3^3+s_1^3s_2s_3^2+s_1^2s_2^3s_3+s_1^3s_2^2s_3$ | -0.145604(1) | -0.245149 |
| 23 | $s_1^2s_2^2s_3^2$ | -0.829799 | 0.254226 |

Other parameters : $z_1$ = 0.736866(-1) ; $z_2$ = -0.188982(-1)
$z_3$ = 0.239406(-2) ; $z_4$ = -0.120142(-3)

*All distances in units of $a_o$ and all coefficients have units such that the energy is given in Hartrees. Numbers in parentheses indicate power of ten.

Table II. Rotationally summed integral cross sections in $Å^2$ for the vibrational excitation $n = 0 \rightarrow n'$ at 10 eV.*

| | $n' = 1$ | $n' = 2$ | $n' = 3$ |
|---|---|---|---|
| This work | 5.885 | 2.244 | 0.613 |
| Schinke, McGuire[1] | 4.00 | 1.239 | 0.557 |

*The indicated reference numbers are those of the text.

FIGURE CAPTIONS

Fig. 1. Interaction potential $V_I$ vs R for r = 0.6 $a_o$, 1.4 $a_o$ and 2.2 $a_o$. Open circles (o): ab initio points of this work; full circles (•): obtained from Giese and Gentry's surface;[3] solid line (————): analytic expression of this work. (a) collinear, $\gamma = 0^o$, (b) perpendicular, $\gamma = 90^o$.

Fig. 2. Schematic illustration of the analytic procedure described in Section III.

Fig. 3. Interaction potential vs r for R = 2 $a_o$, 3 $a_o$, 4 $a_o$ and 5 $a_o$ for collinear geometry, $\gamma = 0^o$. Full line (——): analytical expression of this work; dashed line (- - -): Giese and Gentry's surface.[3] Dots (•): ab initio points of this work.

Fig. 4. Same as Fig. 3, but for perpendicular geometry, $\gamma = 90^o$.

Fig. 5. Transition probabilities for vibrational excitation, $|S^{\ell'}_{0n'}(\gamma)|^2$ for n' = 1 vs partial wave parameter $\ell'$ at 10 eV for the collinear, $\gamma = 0^o$ and the perpendicular, $\gamma = 90^o$ geometries. Full line (——): this work; dashed line (- - -): Schinke and McGuire, Ref. 1.

Fig. 6. Vibrational transition probabilities $P^{n'}$ vs scattering angle $\theta$ for vibrationally inelastic transitions n = 0 → n' = 1, 2 and 3 at 10 eV. Full line (——): this work; dashed line (- - -): Schinke and McGuire, Ref. 1. Experiments (Φ): Hermann et al.[5]

Fig. 7. Rotationally summed differential cross sections for vibrational transitions $n = 0 \rightarrow n' = 0$, 1, 2, and 3 at 10 eV. Full line (——): this work; dashed line (- - -): Schinke and McGuire, Ref. 1. The experiments ($\Phi$) of Hermann et al.[5] are normalized at one point, $\theta \sim 15^{\circ}$, to the vibrationally elastic theoretical results of this work.

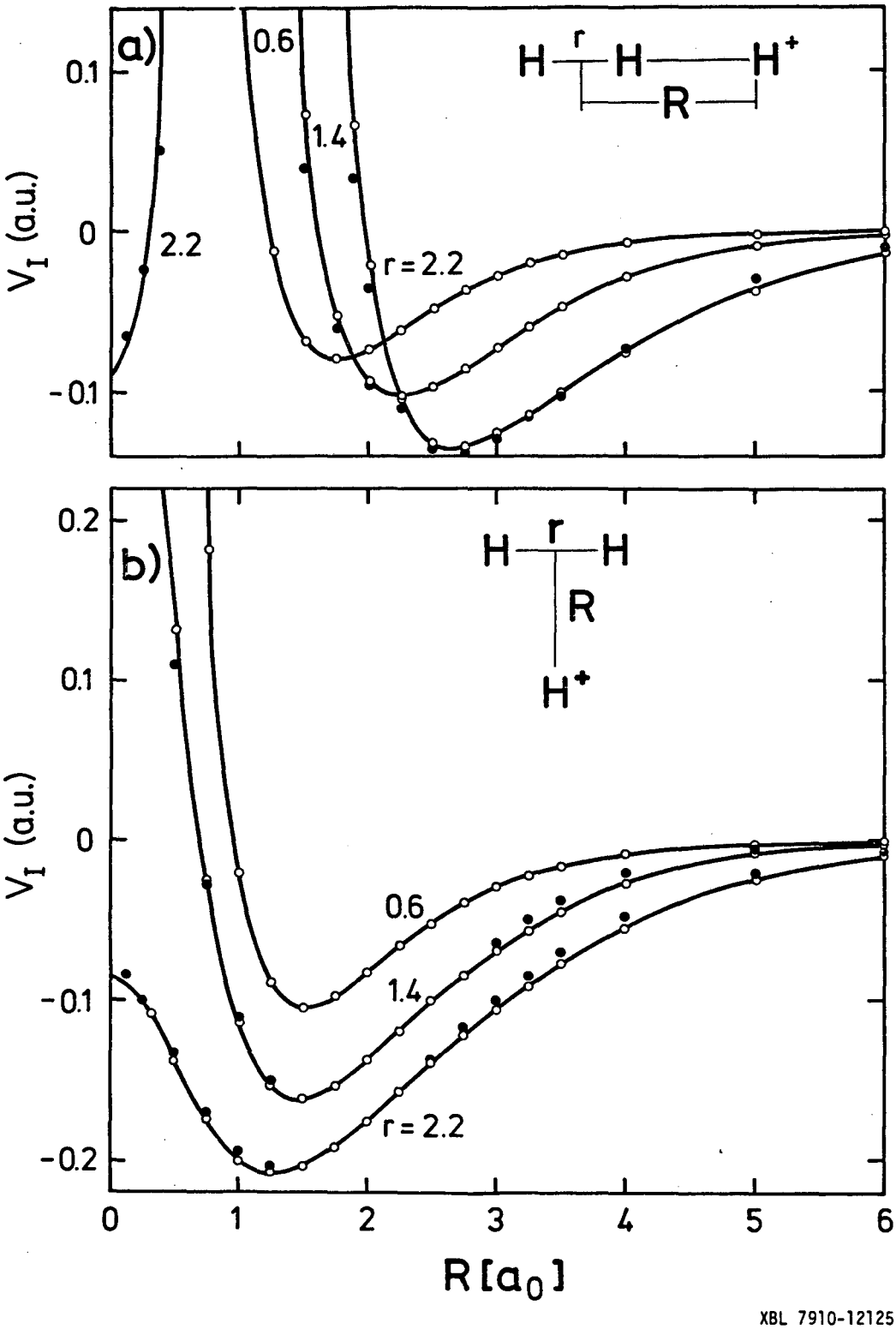


XBL 7910-12125

Fig. 1

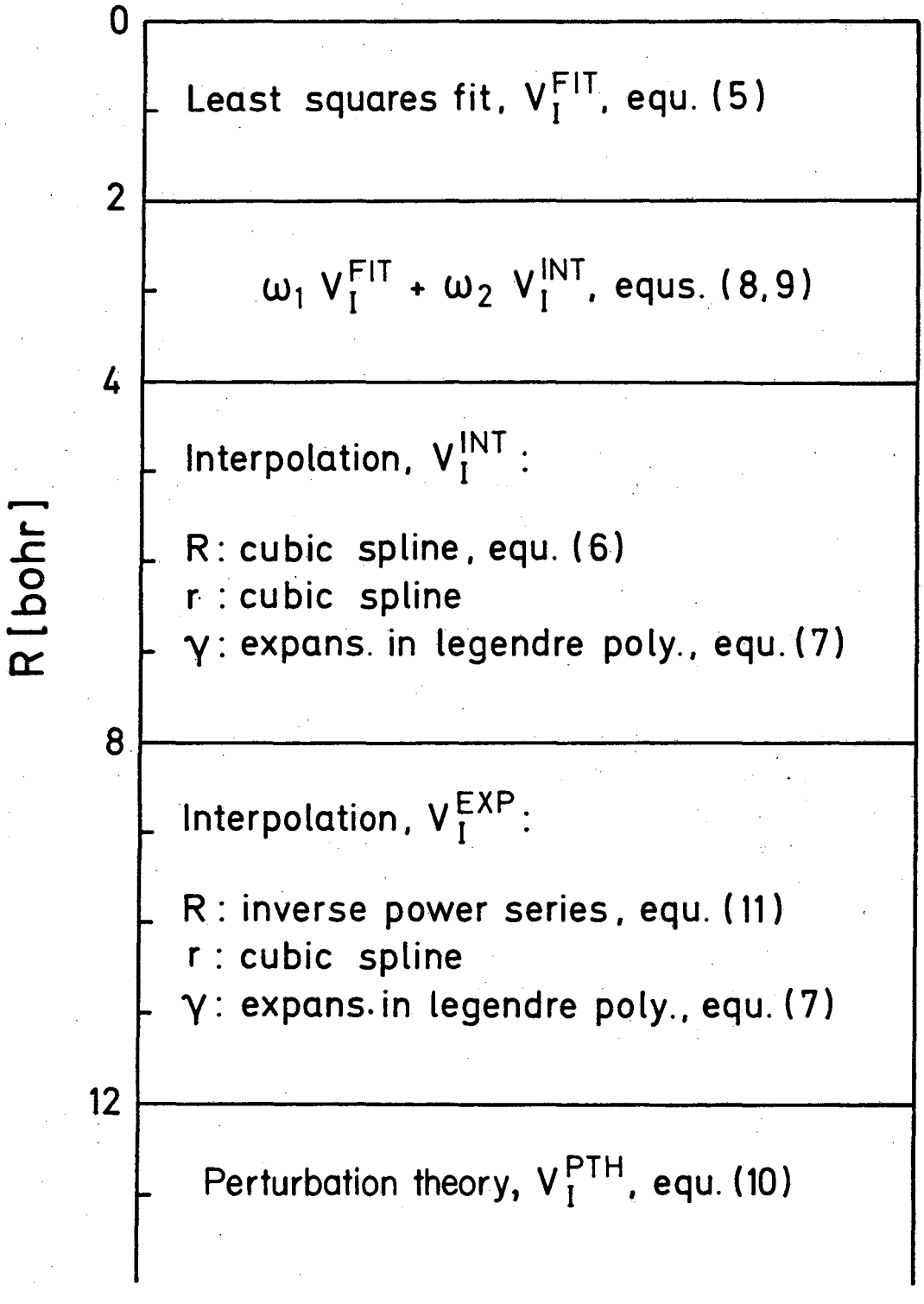


XBL 7910-12126

Fig. 2

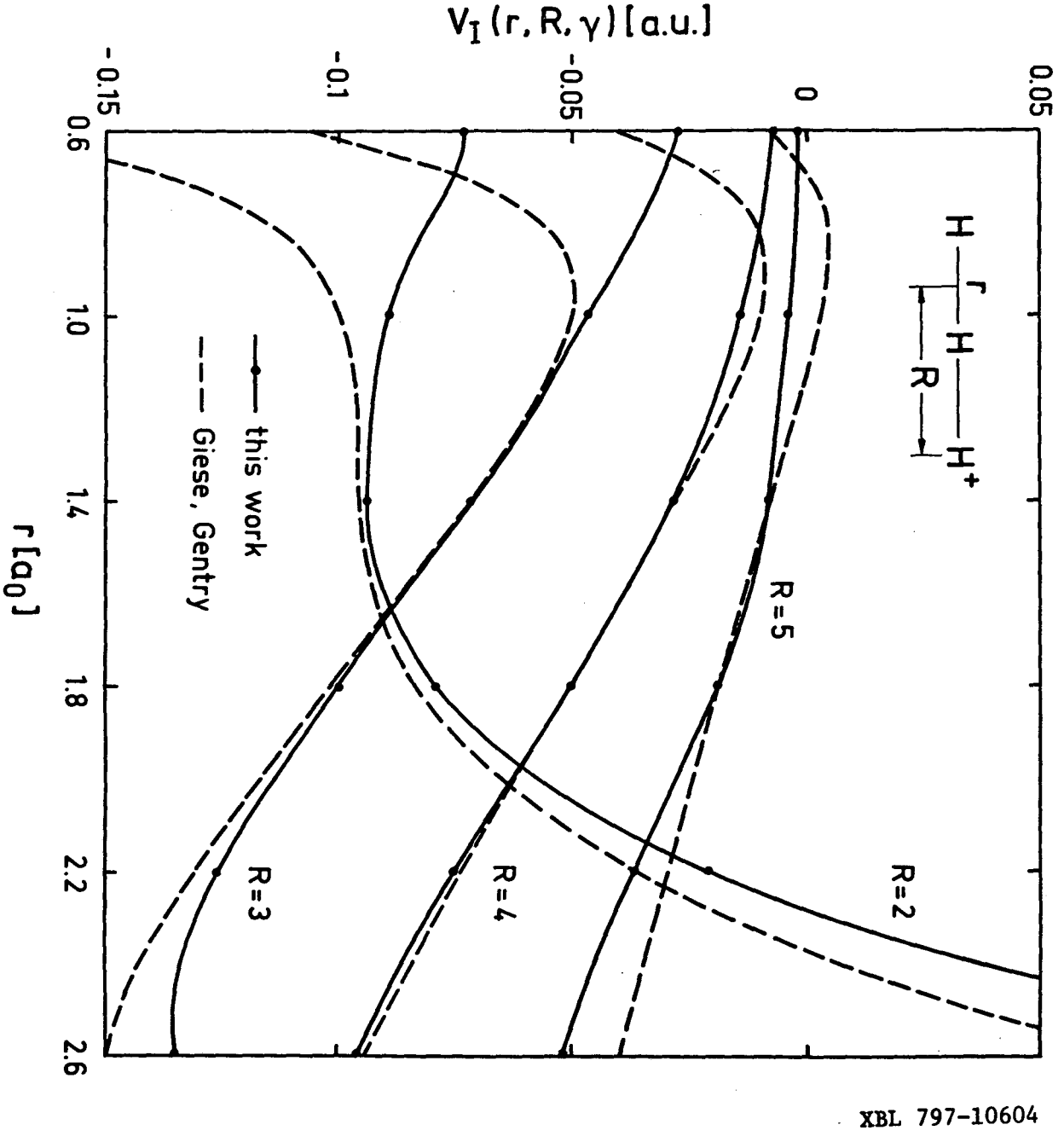


XBL 797-10604

Fig. 3

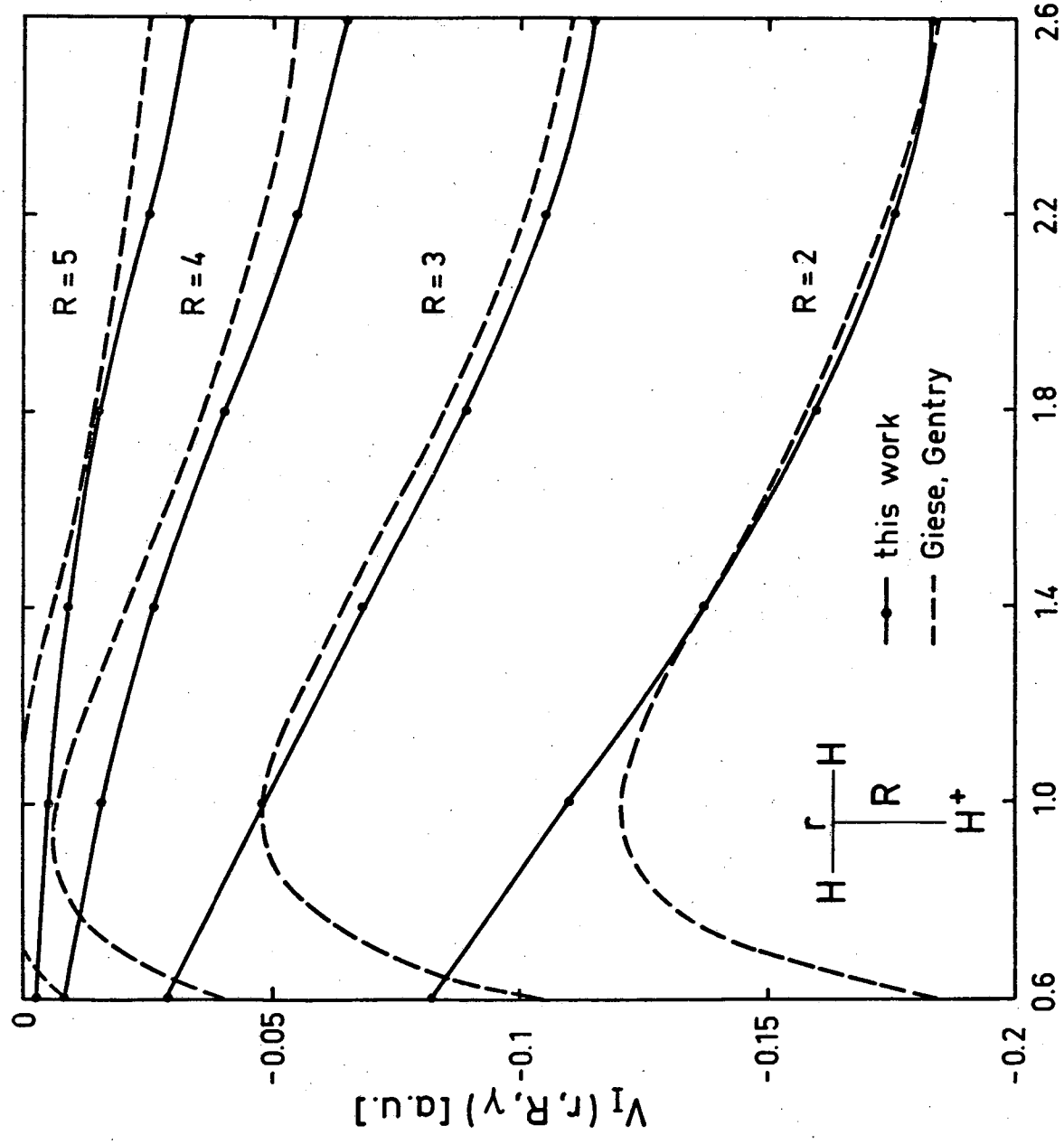


XBL 797-10605

Fig. 4

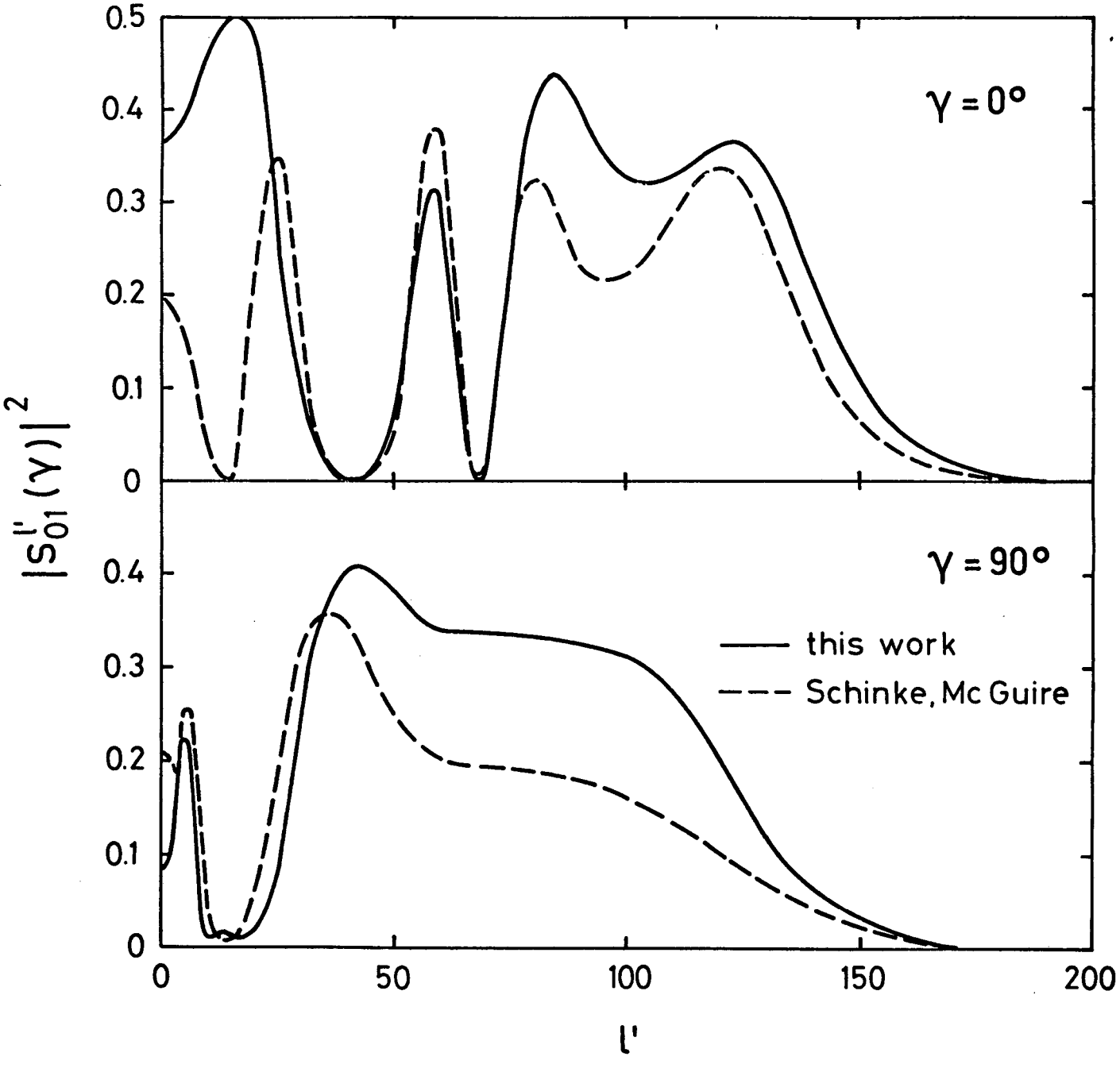


Fig. 5

XBL 797-10606

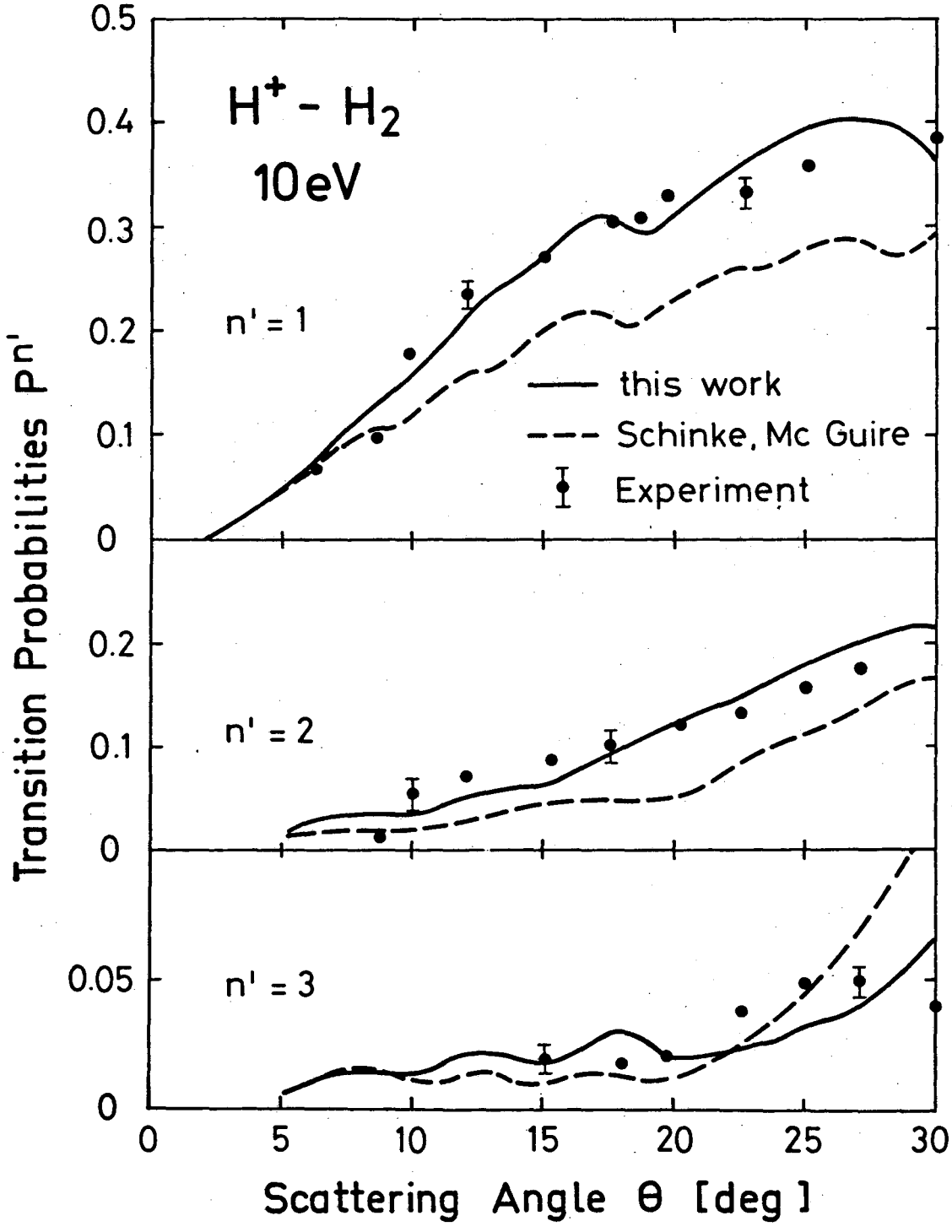


XBL 797-10607

Fig. 6

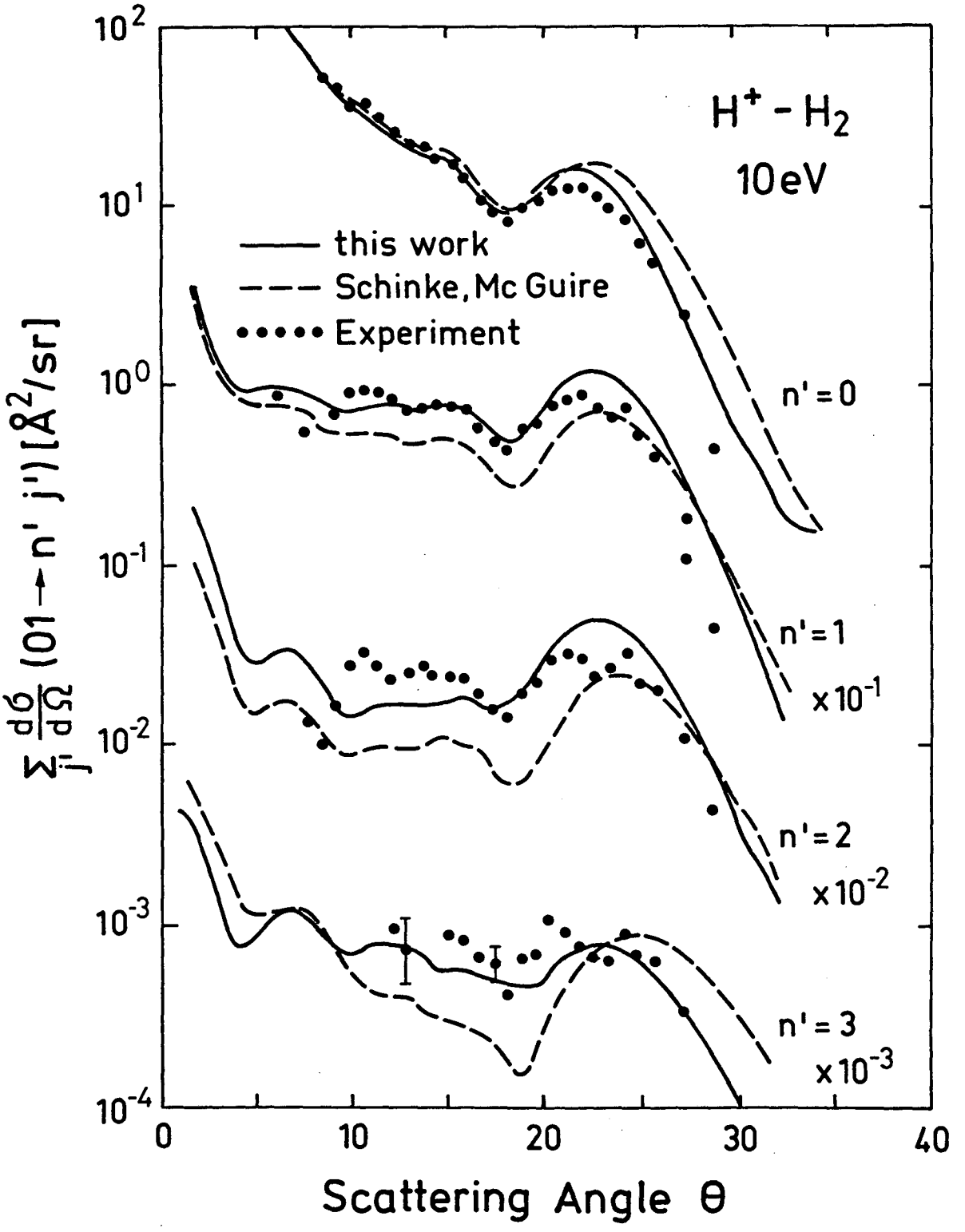


XBL 797-10608

Fig. 7

This report was done with support from the Department of Energy. Any conclusions or opinions expressed in this report represent solely those of the author(s) and not necessarily those of The Regents of the University of California, the Lawrence Berkeley Laboratory or the Department of Energy.

Reference to a company or product name does not imply approval or recommendation of the product by the University of California or the U.S. Department of Energy to the exclusion of others that may be suitable.

*TECHNICAL INFORMATION DEPARTMENT*
*LAWRENCE BERKELEY LABORATORY*
*UNIVERSITY OF CALIFORNIA*
*BERKELEY, CALIFORNIA 94720*